EVIDENCE OF DOUBLE PARTON SCATTERING AT LHCb*

Saliha Bashir†, Agnieszka Oblakowska-Mucha

on behalf of the LHCb Collaboration

AGH University of Science and Technology
al. Mickiewicza 30, 30-059 Kraków, Poland

Received 14 April 2022, accepted 29 April 2022, published online 9 September 2022

Results showing the contribution from Double Parton Scattering were reported by the LHCb experiment based on Run 2 data sample. The production cross section of J/ψ pairs was measured in pp collisions at a centre-of-mass energy $\sqrt{s} = 13$ TeV and compared to theoretical predictions. Pairs of prompt charm hadrons were studied in proton–lead collisions at $\sqrt{s_{NN}} = 8.16$ TeV and confirmed the enhancement of DPS compared to single parton scattering production.

DOI:10.5506/APhysPolBSupp.15.3-A33

1. Introduction

Production of particles at proton–proton (pp) collisions is governed by elementary collisions of partons. Quantum chromodynamics (QCD), the theory of strong interactions, provides a good description of the production of hadrons with large momentum transfer. The nonperturbative effects such as the underlying event, hadronization, and parton showering are subjects of phenomenological models, implemented in dedicated event generators and extensively compared with available data.

The most common mechanism for hard processes in proton–proton collision is Single Parton Scattering (SPS) which involves two partons, one from each proton which undergo hard scattering and produce particles with high transverse momenta. On the other hand, Double Parton Scattering (DPS)

* Presented at the 28th Cracow Epiphany Conference on *Recent Advances in Astroparticle Physics*, Cracow, Poland, 10–14 January, 2022.

† Corresponding author: bashir@agh.edu.pl

occurs if in the same proton–proton collision two partons from the same proton initiate two separate hard scattering processes [1]. DPS becomes more probable and therefore increasingly important at high protons' energies. In addition, in proton–ion collisions, the DPS production might be pronounced due to nuclear matter effects.

The DPS production cross section contains two parton level cross sections (σ_A and σ_B) and the effective cross section (σ_{eff}), which is related to collision geometry and is expected to be independent of the final states, see Eq. (1)

$$\sigma_{\text{DPS}} = \frac{1}{1+\delta_{AB}} \frac{\sigma_A \sigma_B}{\sigma_{\text{eff}}}, \tag{1}$$

where $\delta_{AB} = 1$ if A and B are identical particles and is zero otherwise [2].

1.1. LHCb detector

The LHCb detector is a single arm forward spectrometer covering pseudorapidity range of $2 < \eta < 5$ [3]. The physics program of LHCb is dedicated to study heavy flavor physics and demonstrates excellent capabilities in electroweak and QCD physics. Its aim is to search for evidence of new physics, CP violation, and rare decays of beauty and charm hadrons [4]. The closest detector to the interaction point is the Vertex Locator (VELO) which provides measurements of track coordinates used for the identification of primary vertex and secondary vertex [5]. Tracking detectors before and after a 4 Tm dipole magnet reconstruct the particle's momentum with a relative uncertainty of about 0.5% for low momentum and 1.0% for high momentum (> 200 GeV/c) tracks. The RICH detectors, along with hadron and electron calorimeters, are used for particle identification. Muons are identified in muon chambers which are located at the end of the LHCb spectrometer. The LHCb spectrometer (Fig. 1) with the description of all main subsystems can be found in [4].

By the end of Run 2 despite collecting more data than anticipated, the experimental precision has not reached the theoretical predictions and hence many experimental results remain statistically limited. An increase in the data sample will not only improve the experimental sensitivity but also allow for new theoretical interpretations. Starting from 2022, LHCb plans to take data at an instantaneous luminosity of $2 \times 10^{33}\,\text{cm}^{-2}\,\text{s}^{-1}$ which is 5 times higher compared to Run 2. In order to cope with these conditions LHCb upgraded the DAQ system and installed a purely software-based trigger, the details of which are mentioned in [6]. There is also an upgrade in the sub-detectors: VELO which now consists of 26 tracking layers using pixel technology, and the tracking detectors before and after the magnet are upgraded to Upstream Tracker (UT) and Scintillating Fibers tracker (SciFi), respectively. Further details about the upgrade could be accessed at [7].

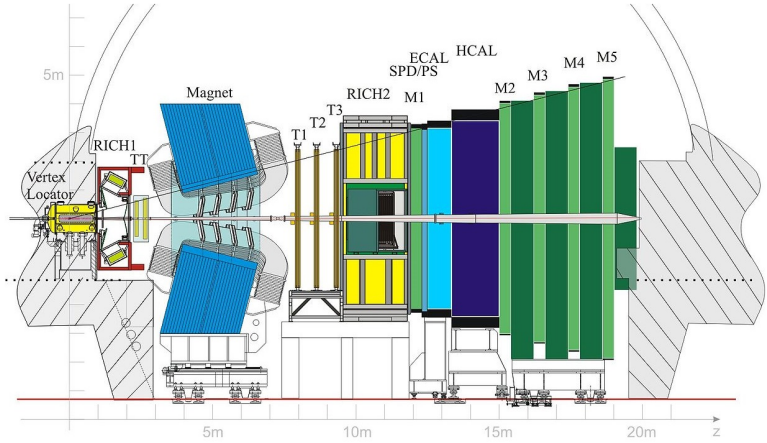

Fig. 1. The scheme of the LHCb spectrometer [4].

2. Double parton scattering in J/ψ pair production at $\sqrt{s} = 13$ TeV

The J/ψ pair production cross section is measured in proton–proton collision at $\sqrt{s} = 13$ TeV using data sample collected by the LHCb experiment corresponding to an integrated luminosity of 279 pb^{-1}. The produced J/ψ pairs are within a rapidity range $2 < \eta < 4.5$ and transverse momentum $p_{\mathrm{T}} < 10$ GeV/c. The inclusive pair production cross section of J/ψ is measured from Eq. (2)

$$\sigma_{J/\psi J/\psi} = \frac{N^{\mathrm{cor}}}{\mathcal{L} \times \mathcal{B}(J/\psi \to \mu^+\mu^-)}\,, \tag{2}$$

where N^{cor} is the signal yield after the efficiency correction, $\mathcal{L}$ is the integrated luminosity (*i.e.* $\mathcal{L} = 279 \pm 11$ pb^{-1}), and $\mathcal{B}(J/\psi \to \mu^+\mu^-)$ is the branching fraction of $J/\psi \to \mu^+\mu^-$ decay which is $(5.961 \pm 0.033)\%$. Software trigger and hardware trigger select high-quality muons. In order to have good track qualities, the muons are required to have momentum in the range of $p_{\mathrm{T}} < 650$ MeV/c, $6 < p < 200$ GeV/c, and pseudorapidity in the range of $2 < \eta < 5$. The four muons should be produced from the same primary vertex (PV) to reduce the duplicate and multiple candidates. The signal yield is obtained by performing an extended unbinned maximum likelihood fit to efficiency corrected two-dimensional $M(\mu_1^+\mu_1^-)$ and $M(\mu_2^+\mu_2^-)$ mass distribution. Labels 1 and 2 are assigned randomly to the two J/ψ candidates. The signal mass distribution for each dimension is described by the Gaussian function with power-law tails. The combinatorial background is modelled by the exponential function. The fit projections on $M(\mu_1^+\mu_1^-)$ and $M(\mu_2^+\mu_2^-)$ are shown in Fig. 2

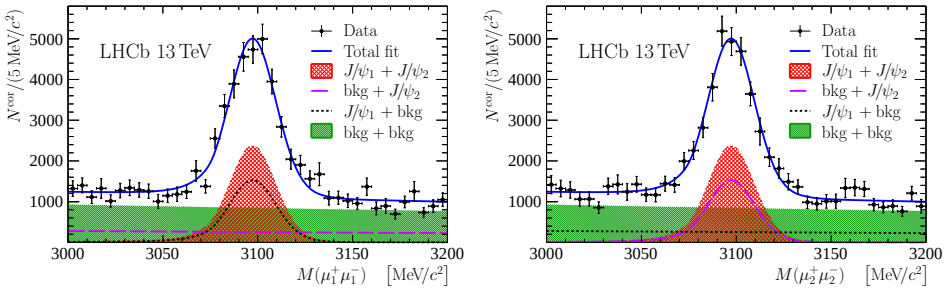

Fig. 2. The figure shows the projection of the fit to the efficiency corrected distribution on $M(\mu_1^+\mu_1^-)$ and $M(\mu_2^+\mu_2^-)$. The larger peak represents the data with error bars. The smaller peak represents the signal distribution. The horizontal line shows pure combinatorial background [8].

The corrected yield of the J/ψ pair is $N^{\rm cor} = (15.8 \pm 1.1) \times 10^3$ [8]. The J/ψ pair production cross section, where both pairs of J/ψ are in the region, $2.0 < y < 4.5$ and $p_{\rm T} < 10$ GeV/c is measured to be

$$\sigma(J/\psi J/\psi) = 15.2 \pm 1.0(\text{stat.}) \pm 0.9(\text{syst.})\ \text{nb}\,.$$

The differential cross section of J/ψ pair production as a function of several kinematic variables is compared to various theoretical predictions. The most significant contribution of DPS is obtained when the differential cross section is plotted with respect to the difference in rapidity between two J/ψ mesons ($|\Delta y|$) and mass, as shown in Fig. 3. In the distribution, where cross section is plotted as a function of $|\Delta y|$, there is a contribution from the DPS model above $|\Delta y| > 1.5$. For the distribution of cross section plotted as a function of mass, the same models are used for SPS and DPS, and there is

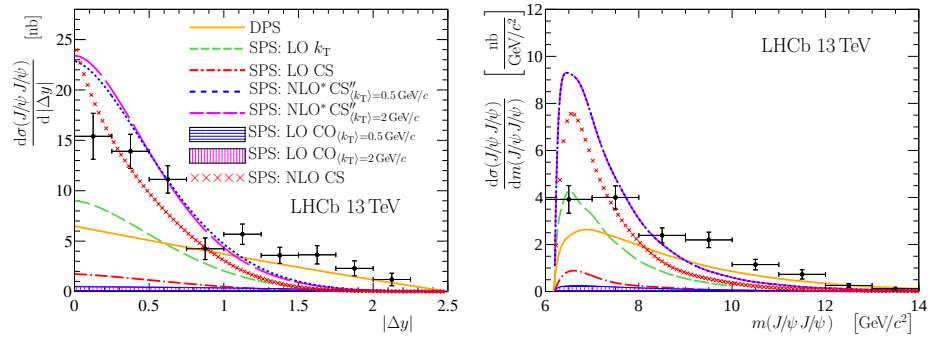

Fig. 3. Comparison of measurement and theoretical predictions for differential cross section as a function of the difference in rapidity between the two J/ψ mesons $|\Delta y|$ (left), and differential cross section as a function of $m(J/\psi\ J/\psi)$ (right) [8].

an apparent contribution from DPS for mass above 11 GeV/c^2. Neither the DPS model nor any SPS models can simultaneously describe the measured cross section and the differential shapes, however, a fit to differential cross section using the sum of DPS and SPS models together indicates a significant DPS contribution.

3. Enhancement of double parton scattering in *p*–Pb collision

The production of two open-charm hadrons D_1 and D_2 where $D_{1,2} = D^0, D^+, D_s^+$ and J/ψ meson pairs is of particular interest in the study of Single Parton Scattering (SPS) and Double Parton Scattering (DPS). The data used in this study is from the LHCb experiment collected at a low interaction rate with two different beam configurations: proton–lead (pPb) and lead–proton (Pbp), the former is when the particles are analysed in the direction of proton beam and the latter *vice versa*. The integrated luminosity corresponding to both the configurations *i.e.* pPb(Pbp) is 12.2 ± 0.3 nb^{-1} (18.6$\pm$0.5 nb^{-1}). The charm hadrons are reconstructed via decays of $D^0 \to K^-\pi^+$, $D^+ \to K^-\pi^+\pi^+$, $D_s^+ \to K^-K^+\pi^+$ and $J/\psi \to \mu^+\mu^-$. For the offline selection, the pions and kaons are required to have momentum $p > 3$ GeV/c, whereas the muons $p > 6$ GeV/c and $p_{\rm T} > 750$ MeV/c. Cross section is calculated based on Eq. (2), where branching fractions for both charm hadron decays are considered. The correlation of kinematics between the two charm hadrons pairs produced is investigated from their relative azimuthal angle ($\Delta\phi$). Figure 4 shows the invariant mass distribution for the pPb configuration (left) and Pbp configuration (right). For both pairs $D^0\bar{D}^0$, the mass distribution is compatible with data and PYTHIA 8 simulations [9].

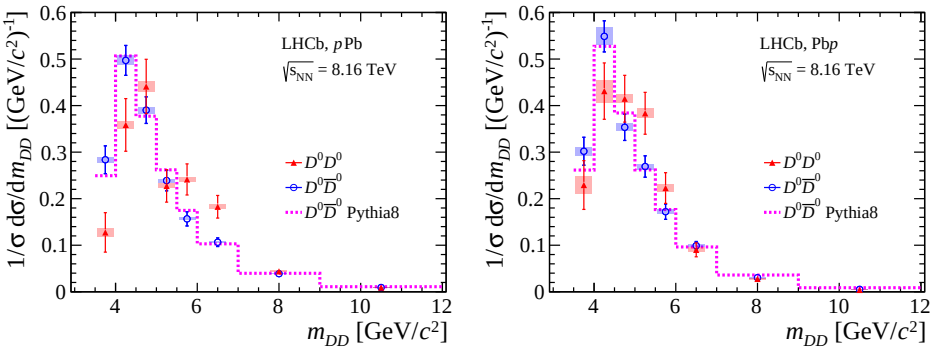

Fig. 4. The invariant mass distribution for two charm hadrons produced D^0D^0 and $D^0\bar{D}^0$, and PYTHIA 8 simulations. Filled boxes represent systematic uncertainties, bars represent statistical uncertainties [9].

The $\Delta\phi$ distribution shown in Fig. 5 is obtained with (top) and without (bottom) the requirement on $p_{\mathrm{T}} > 2$ GeV/c. Without the requirement, the distribution is uniform for both the pairs and is consistent with PYTHIA 8 simulations, with the observation $D^0\bar{D}^0$ favors $\Delta\phi \sim 0$, whereas for D^0D^0 is still compatible with being flat and PYTHIA 8 simulations are inconsistent for both pairs. Distributions for D^0D^0 are consistent with a large DPS contribution. The effective cross sections are evaluated from Eq. (1) in which the cross sections for D^0D^0 and J/ψ are used assuming solely the DPS production by extrapolating the results from pp and scaling them to the Pb mass number 208. These results are the first measurement for the charm pair production in proton–lead collisions at $\sqrt{s_{NN}} = 8.16$ TeV. The results do confirm the expectation that DPS in pPb collisions is enhanced by a factor of 3 when compared to the SPS production [10]. However, the σ_{eff} shows a difference in the level of DPS enhancement for the forward and backward configurations which might need further investigation [9].

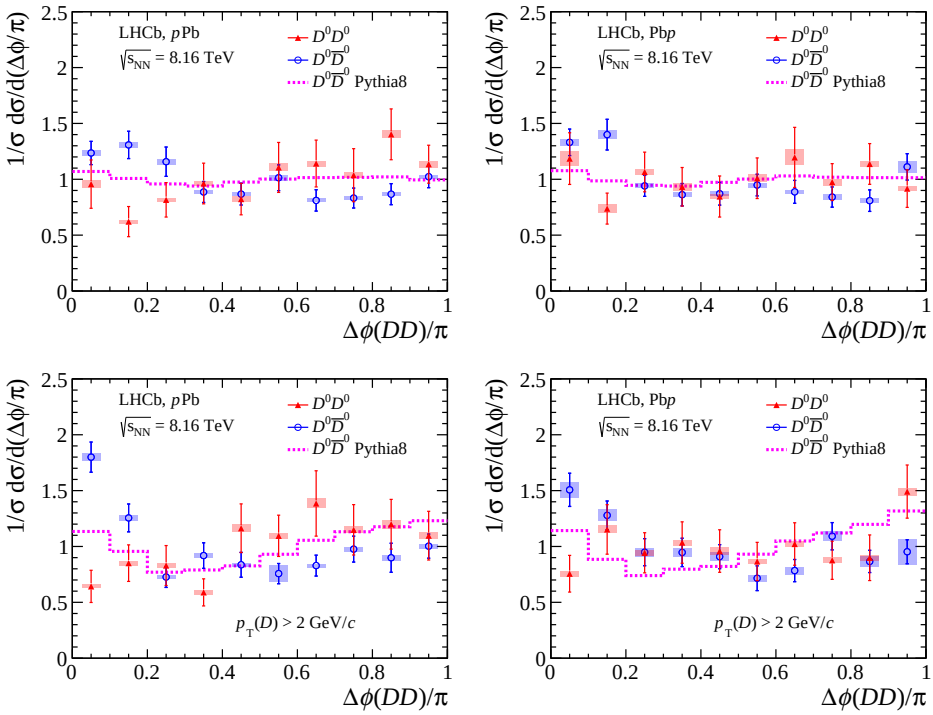

Fig. 5. $\Delta\phi$ distribution for D^0D^0 and $D^0\bar{D}^0$ for pPb data (left) and Pbp data (right). The bottom plots also have the requirement on $p_{\mathrm{T}} > 2$ GeV/c. Filled boxes represent systematic uncertainties, bars represent statistical uncertainties [9].

4. Conclusion

LHCb results show a potential to study Double parton Scattering (DPS). The results reported indicate a significant contribution of DPS in proton–proton collision at $\sqrt{s} = 13$ TeV and in proton-lead collision at $\sqrt{s_{NN}} = 8.16$ TeV. A large DPS contribution results in smaller values of σ_{eff} which when compared to the σ_{eff} values measured previously by the LHCb Collaboration are even smaller in the process of multiple associated heavy quark production [11]. The results presented for proton–lead collisions are the first direct observation of enhancement of DPS, in which the difference in σ_{eff} values for pPb and Pbp configurations could be further investigated with future samples produced by the upgraded LHCb detector for Run 3.

This work was partially supported by the National Research Centre, Poland (NCN), grant No. UMO-2019/35/O/ST2/00546.

REFERENCES

[1] M. Diehl, J.R. Gaunt, «Chapter 2: Double Parton Scattering Theory Overview», *Adv. Ser. Direct. High Energy Phys.* **29**, 7 (2018), arXiv:1710.04408 [hep-ph].

[2] A. Del Fabbro, D. Treleani, «Scale factor in double parton collisions and parton densities in transverse space», *Phys. Rev. D* **63**, 057901 (2001), arXiv:hep-ph/0005273.

[3] LHCb Collaboration (A.A. Alves Jr, *et al.*), «The LHCb Detector at the LHC», *J. Instrum.* **3**, S08005 (2008).

[4] R. Aaij *et al.*, «LHCb Detector Performance», *Int. J. Mod. Phys. A* **30**, 1530022 (2014).

[5] R. Aaij *et al.*, «Performance of the LHCb Vertex Locator», *J. Instrum.* **9**, P09007 (2014).

[6] P. Seyfert, «Tracking, Vertexing and data handling strategy for the LHCb upgrade», *PoS* **(Vertex2017)**, 039 (2018).

[7] O. Steinkamp, «LHCb Upgrades», *J. Phys.: Conf. Ser.* **1271**, 012010 (2019).

[8] R. Aaij *et al.*, «Measurement of the J/ψ pair production cross-section in pp collisions at $\sqrt{s} = 13$ TeV», *J. High Energy Phys.* **2017**, 47 (2017).

[9] R. Aaij *et al.*, «Observation of Enhanced Double Parton Scattering in Proton–Lead Collisions at $\sqrt{s} = 8.16$ TeV», *Phys. Rev. Lett.* **125**, 212001 (2020).

[10] I. Helenius, H. Paukkunen, «Double D-meson production in proton–proton and proton–lead collisions at the LHC», *Phys. Lett. B* **800**, 135084 (2020).

[11] R. Aaij *et al.*, «Observation of double charm production involving open charm in pp collisions at $\sqrt{s} = 7$ TeV», *J. High Energy Phys.* **1206**, 141 (2012), *Addendum ibid.* **1403**, 108 (2014).